Kinase-dead ATM protein causes genomic instability and early embryonic lethality in mice

Kenta Yamamoto,[1,2,4] Yunyue Wang,[1,2] Wenxia Jiang,[1,2] Xiangyu Liu,[1,2] Richard L. Dubois,[1,2] Chyuan-Sheng Lin,[2] Thomas Ludwig,[1,2] Christopher J. Bakkenist,[5,6] and Shan Zha[1,2,3]

[1]Institute for Cancer Genetics, [2]Department of Pathology and Cell Biology, Herbert Irving Comprehensive Cancer Center, [3]Division of Pediatric Oncology, Department of Pediatrics, Columbia University Medical Center, and [4]Graduate program of Pathobiology and Molecular Medicine, College of Physicians and Surgeons, Columbia University, New York, NY 10032
[5]Department of Radiation Oncology and [6]Department of Pharmacology and Chemical Biology, Hillman Cancer Center, University of Pittsburgh School of Medicine, Pittsburgh, PA 15213

Ataxia telangiectasia (A-T) mutated (ATM) kinase orchestrates deoxyribonucleic acid (DNA) damage responses by phosphorylating numerous substrates implicated in DNA repair and cell cycle checkpoint activation. A-T patients and mouse models that express no ATM protein undergo normal embryonic development but exhibit pleiotropic DNA repair defects. In this paper, we report that mice carrying homozygous kinase-dead mutations in *Atm* ($Atm^{KD/KD}$) died during early embryonic development. $Atm^{KD/-}$ cells exhibited proliferation defects and genomic instability, especially chromatid breaks, at levels higher than $Atm^{-/-}$ cells. Despite this increased genomic instability, $Atm^{KD/-}$ lymphocytes progressed through variable, diversity, and joining recombination and immunoglobulin class switch recombination, two events requiring nonhomologous end joining, at levels comparable to $Atm^{-/-}$ lymphocytes. Together, these results reveal an essential function of ATM during embryogenesis and an important function of catalytically inactive ATM protein in DNA repair.

Introduction

Mutations in *ataxia telangiectasia* (*A-T*) *mutated* (*ATM*) cause the autosomal recessive disorder A-T, a neurodegenerative disease that is often associated with immunodeficiency, genomic instability, and predisposition to cancers (Lavin, 2008). Classical A-T is almost always caused by *ATM* mutations associated with undetectable ATM protein levels (Gilad et al., 1996; Lakin et al., 1996; Lavin, 2008). Mouse models that express no ATM protein recapitulate most of the human A-T phenotypes with the exception of the spontaneous progressive cerebella atrophy (Barlow et al., 1996; Xu and Baltimore, 1996; Herzog et al., 1998; Borghesani et al., 2000).

ATM kinase exists as inert dimers or higher order oligomers in unstressed cells and is converted to active monomers by agents that induce DNA double-strand breaks (DSBs; Bakkenist and Kastan, 2003; Carson et al., 2003; Uziel et al., 2003; Lee and Paull, 2004, 2005). Although autophosphorylation of ATM at S1981 (corresponding to S1987 in mouse) has been used as a reliable marker of ATM activation, whether S1981 phosphorylation is required for ATM activation is unclear. Expression of human ATM protein containing S1981A mutation fails to restore all ATM function in A-T cells (Bakkenist and Kastan, 2003; Lavin, 2008). However, both purified wild-type (WT) and S1981A mutated human ATM proteins can be activated in vitro (Lee and Paull, 2004). Furthermore, mouse models bearing a homozygous S1987A mutation or S1987A plus two additional autophosphorylation site mutations (corresponding to human S367A and S1893A) have no discernable defects in ATM activation (Pellegrini et al., 2006; Daniel et al., 2008).

As a master regulator of DNA damage responses (Bhatti et al., 2011), ATM has been implicated in both nonhomologous end joining (NHEJ) and homologous recombination (HR), the two principal DNA DSB repair pathways.

Correspondence to Shan Zha: sz2296@columbia.edu

Thomas Ludwig's current address is Dept. of Molecular and Cellular Biochemistry, Ohio State University Wexner Medical Center, Columbus, OH 43210.

Abbreviations used in this paper: A-T, ataxia telangiectasia; ATM, A-T mutated; ATR, A-T and Rad3 related; CSR, class switch recombination; DSB, double-strand break; ES, embryonic stem; hCG, human chorionic gonadotropin; HR, homologous recombination; KD, kinase dead; NeoR, neomycin resistant; NHEJ, nonhomologous end joining; PE, phycoerythrin; PKcs, protein kinase catalytic subunit; T-FISH, telomere FISH; V(D)J, variable, diversity, and joining; WT, wild type.

The Rockefeller University Press $30.00
J. Cell Biol. Vol. 198 No. 3 305–313
www.jcb.org/cgi/doi/10.1083/jcb.201204098

NHEJ functions throughout the cell cycle. HR is most active in S and G2 phases of the cell cycle, when a homologous template is available. Developing lymphocytes undergo variable, diversity, and joining (V(D)J) recombination and immunoglobulin class switch recombination (CSR), two events that require NHEJ for completion (Rooney et al., 2004). Loss of ATM compromises both chromosomal V(D)J recombination (Borghesani et al., 2000; Bredemeyer et al., 2006; Huang et al., 2007; Callén et al., 2009a; Zha et al., 2011a) and CSR (Lumsden et al., 2004; Reina-San-Martin et al., 2004; Franco et al., 2006), indicating that ATM has an important function in NHEJ. ATM-deficient cells are also hypersensitive to the loss of PARP1/2 function (Ménisser-de Murcia et al., 2001; Huber et al., 2004), suggesting that ATM has an important function in HR. In addition, ATM deficiency is synergistically lethal with several other mutations that compromise the HR pathway (e.g., Nbs1, A-T and Rad3 related [ATR], and FanG; Williams et al., 2002; Kennedy et al., 2007; Murga et al., 2009).

Selective inhibitors targeting ATM kinase activity have been developed and widely used (Hickson et al., 2004; Rainey et al., 2008; White et al., 2008). Although these inhibitors generally recapitulate the effects of ATM protein deficiency (Bredemeyer et al., 2006; Callén et al., 2009b; Zha et al., 2011a), recent studies have identified DNA repair defects in cells treated with ATM kinase inhibitors that are not observed in ATM-null cells, suggesting additional activities of the kinase-inhibited ATM protein (White et al., 2010; Gamper et al., 2012). Here, we show that in contrast to the normal development of ATM-null mice, mice bearing mutations that result in the normal expression of a kinase-dead (KD) ATM (ATM-KD) protein, D2880A/N2885K (corresponding to D2870A/N2875K in humans; Canman et al., 1998), die during early embryonic development.

Results and discussion

Atm$^{KD/KD}$, but not *Atm*$^{+/KD}$ mice, die during early embryonic development

To generate mice expressing a KD ATM protein, we introduced the previously described D2880A/N2885K (corresponding to D2870A/N2875K in humans; Canman et al., 1998; Bakkenist and Kastan, 2003) double mutation in the sequence encoding the conserved catalytic loop (Fig. 1 A) of the murine *Atm* gene along with a floxed neomycin-resistant (NeoR) cassette (referred to as ATM KDN for the presence of NeoR cassette; Fig. 1 B). We selected the D2870A/N2875K double mutation because it was fully characterized for normal protein expression and the absence of kinase activity (Canman et al., 1998; Bakkenist and Kastan, 2003). Six targeted clones were identified by Southern blot analyses (Fig. 1 C), and the mutations were verified in four clones by genomic sequencing. Two independent targeted clones were injected for germline transmission. *Atm*$^{+/KDN}$ chimeras were then bred with sperm-specific ProtamineCre transgenic mice (O'Gorman et al., 1997) to induce recombination between the loxP sites flanking the *NeoR* to generate the *Atm*$^{+/KD}$ mice, in which the KD, *Atm*^{KD}, allele is transcribed and expressed from the endogenous *Atm* promoter.

Atm$^{+/KD}$ mice are normal in size, fertile, and have no detectable defects in lymphocyte development (Fig. S1, A and B). However, no *Atm*$^{KD/KD}$ mice were identified in >100 pups generated by breedings between *Atm*$^{+/KD}$ mice ($P = 4.0 \times 10^{-8}$ for chi-squared test; Fig. 1 D), indicating embryonic lethality. This was unexpected because *Atm*$^{-/-}$ mice were generated at the roughly Mendelian ratio ($P = 0.16$ for chi-squared test; Fig. 1 E). Timed heterozygous crosses further revealed that no live *Atm*$^{KD/KD}$ embryos could be found ($P = 0.0056$ for chi-squared test; Fig. 1 D) even at embryonic day 9.5–10.5 (E9.5–10.5), indicating early embryonic lethality. We note that the embryonic lethality of KD ATM protein is not caused by a classical dominant-negative mechanism because *Atm*$^{+/KD}$ mice and cells that express both ATM-WT and ATM-KD proteins have no discernable phenotype.

Atm$^{KD/-}$ embryonic stem (ES) cells have greater genomic instability than *Atm*$^{-/-}$ cells

To explore the causes of developmental failure in *Atm*$^{KD/KD}$ mice, we generated *Atm*$^{KD/-}$ ES cells and control *Atm*$^{+/+}$ and *Atm*$^{-/-}$ cells. To circumvent the embryonic lethality, we first derived *Atm*$^{KDN/C}$ ES cells. The previously characterized *Atm* conditional allele (*Atm*^{C}) behaves as the WT allele and can be efficiently converted to a null (*Atm*$^{-}$) allele upon Cre-mediated recombination (Zha et al., 2008, 2011b). We obtained six independent *Atm*$^{KDN/C}$ clones and three control *Atm*$^{+/C}$ clones. *Atm*$^{KD/-}$ ES cells were then generated by infecting *Atm*$^{KDN/C}$ cells with adenovirus expressing Cre recombinase. Although all 24 Cre-transduced *Atm*$^{+/C}$ clones were genotyped as *Atm*$^{+/-}$, indicating efficient recombination, only 2 of the 96 Cre-transduced *Atm*$^{KDN/C}$ clones were genotyped as *Atm*$^{KD/-}$, implying that *Atm*$^{KD/-}$ cells have growth and/or survival defects. Western blot analysis verified that ATM-KD protein is expressed at levels comparable with WT endogenous ATM proteins in *Atm*$^{KD/-}$ ES cells (Fig. 2 A). However, two independently derived *Atm*$^{KD/-}$ ES cell lines grew significantly slower than both *Atm*$^{-/-}$ ES and *Atm*$^{+/+}$ ES cells, which grew at comparable rates (Fig. 2 B).

We proceeded to measure spontaneous genomic instability in *Atm*$^{+/+}$, *Atm*$^{KD/-}$, and *Atm*$^{-/-}$ ES cells using telomere FISH (T-FISH) assays (Franco et al., 2006; Zha et al., 2008). Under regular growth conditions, ~30% metaphases derived from *Atm*$^{KD/-}$ ES cells had spontaneous cytogenetic abnormalities, whereas only 18% of those derived from *Atm*$^{-/-}$ cells and <2% of those derived from WT cells showed such abnormalities (Fig. 2, C and E). In contrast to the predominant chromosome breaks in *Atm*$^{-/-}$ ES cells (Fig. 2, D and E; Franco et al., 2006; Zha et al., 2008), the cytogenetic aberrations in *Atm*$^{KD-}$ ES cells were evenly distributed between chromosome (break involving both sister chromatids) and chromatid (breaks involving one of the two sister chromatids) breaks, with the most dramatic increase observed in chromatid breaks (Fig. 2, D and E; and Fig. S2 C). Although chromosome breaks are derived primarily from DSBs that arise during the G1 phase of the cell cycle, chromatid breaks often result from DSBs in S and G2 phases of the cell cycle, when HR is most active. Together, these results suggest that the physical presence of ATM-KD inhibits

A

Kinase Dead Mutation at the Catalytic Loop of ATM

```
92510 GGA CTT GGC GAC AGG CAC GTA CAG AAT ATC TTG - WT mouse Genomic
8768- GGA CTT GGC GAC AGG CAC GTA CAG AAT ATC TTG - WT mouse mRNA
Mouse- G   L   G   D   R   H   V   Q   N   I   L  - WT Protein
Human- G   L   G   D   R   H   V   Q   N   I   L  -D2870 /N2875  WT protein
Human- G   L   G   A   R   H   V   Q   K   I   L  -D2870A/N2875K KD Protein
Mouse- G   L   G   A   R   H   V   Q   K   I   L  -D2880A/N2885K KD Protein
8768- GGA CTT GGC GCC AGG CAC GTA CAG AAA ATC TTG - KD mouse mRNA
92510 GGA CTT GGC GCC AGG CAC GTA CAG AAA ATC TTG - KD mouse Genomic
```

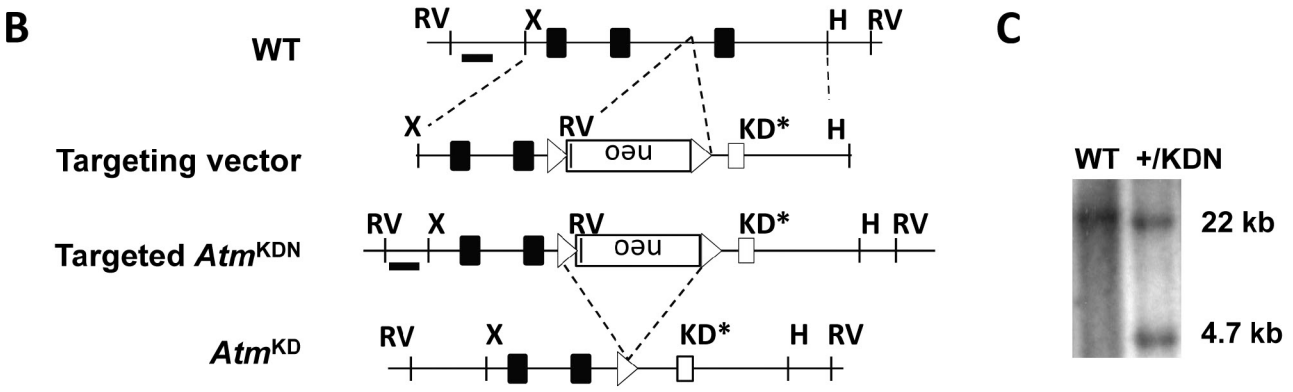

D

Total	*Atm*$^{+/+}$	*Atm*$^{+/KD}$	*Atm*$^{KD/KD}$	Absorbs	Total	p-value
E9.5-10.5	4	18	0	3	22	0.0056
Live Birth	35	67	0	-	102	4.0×10^{-8}

E

Total	*Atm*$^{+/+}$	*Atm*$^{+/-}$	*Atm*$^{-/-}$	Total	p-value
Live Birth	19	27	9	55	0.16
Exp No	13.75	27.5	13.75	-	

Figure 1. **Generation of the *Atm*^{KD} allele.** (A) The corresponding sequence of the catalytic loop of human and mouse ATM kinase are aligned, and the mutated residues are underlined. Gray shade covers the corresponding WT and mutated sequences in human ATM protein. (B) The schematic diagram represents the murine *Atm* locus (top), targeting vector (second row), targeted allele (*Atm*^{KDN}, third row), and the neomycin (neo)-deleted mutant allele (*Atm*^{KD}, bottom). The 5′ probe is marked as a black line. The exons and loxP sites are shown as solid boxes and open triangles, respectively. The exon containing the KD mutation is marked as an open box. Restriction site designations are as follows: X, XhoI; RV, EcoRV; H, HindIII. The map is not drawn to scale. (C) Southern Blot analyses of EcoRV-digested DNA from representative *Atm*$^{+/+}$ (WT) and *Atm*$^{+/KDN}$ ES cells. (D and E) Genotype of embryos and live offspring obtained from timed intercrossing between *Atm*$^{+/KD}$ mice (D) and *Atm*$^{+/-}$ mice (E). Compared with the expected Mendelian frequency, the χ^2 test p-values are 0.0056 for E9.5–10.5 *Atm*$^{KD/KD}$ embryos and 4.01×10^{-8} for *Atm*$^{KD/KD}$ and 0.16 for *Atm*$^{-/-}$ mice at birth. Exp, expected.

DNA repair, likely HR, in a manner that does not occur in the absence of ATM protein. When we expressed mEOS2-ATM in cells in which the endogenous ATM protein was disrupted, both WT and KD ATM are recruited to the site of DNA damage and retained there for ≥5 min (Fig. S2 B). Similar results were obtained in two previous studies (Barone et al., 2009; Davis et al., 2010). Furthermore, previous studies have identified both replication-related DNA repair defects and increased chromatid breaks in cells treated with selective ATM kinase inhibitors (White et al., 2010; Gamper et al., 2012) but not in ATM-null

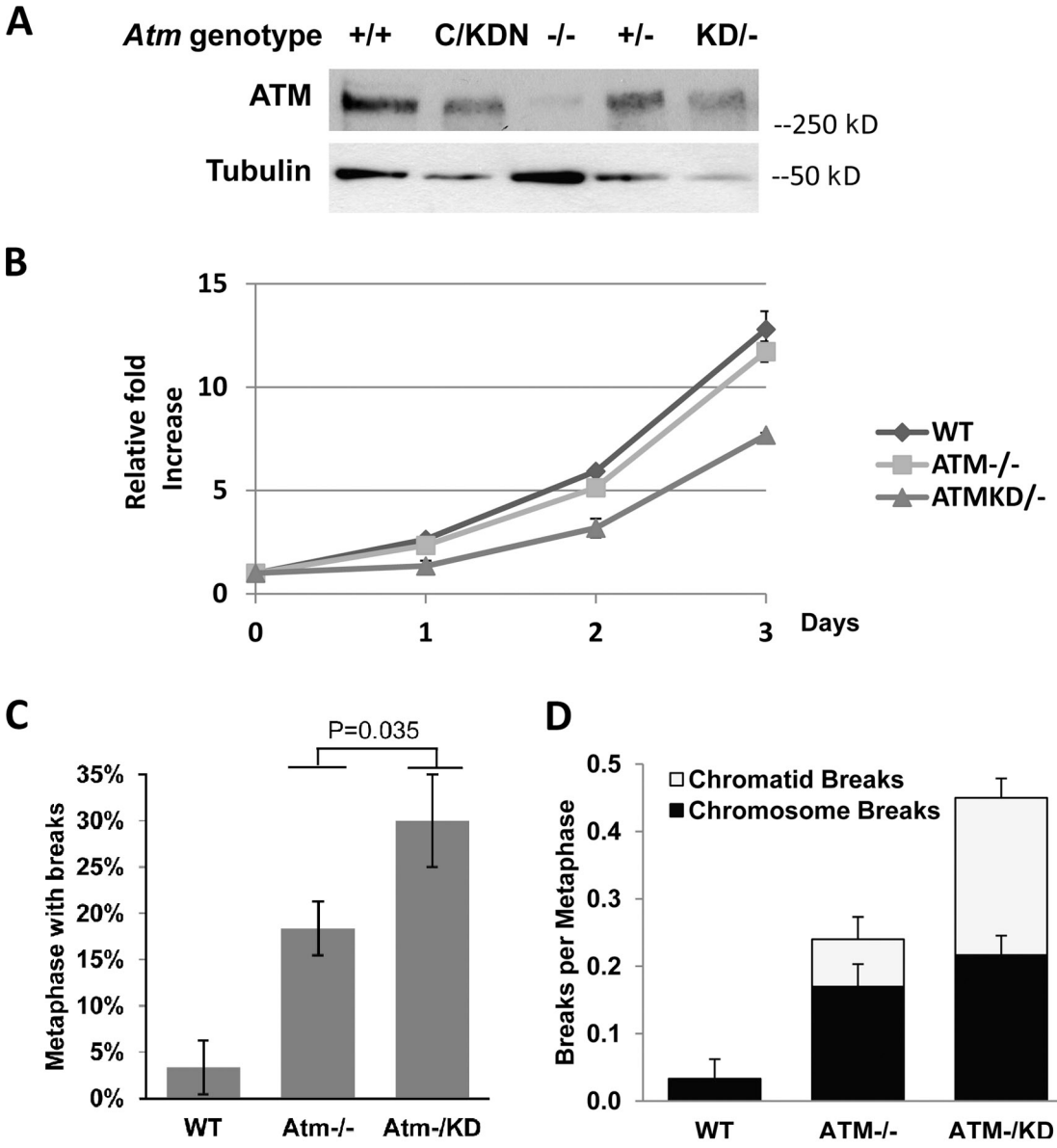

E

	No. Metaphase	Abnormal MP	Ab. MP%	Std.Er	Chs. Br.	Chs/MP	Std.Er	Cht. Br.	Cht/MP	Std.Er
WT	80	1	1.3%	2.9%	1	0.01	0.03	0	0.00	0.00
ATM$^{-/-}$	60	11	18.3%	2.9%	10	0.17	0.03	4	0.07	0.03
ATM$^{-/KD}$	60	18	30.0%	5.0%	11	0.18	0.03	14	0.23	0.03

Figure 2. **Proliferation defects and increased genomic instability in $Atm^{KD/-}$ ES cells.** (A) Western blot analysis of total protein (50 µg) for mouse ATM (MAT3; Sigma-Aldrich) and α-tubulin (EMD) in WT, $Atm^{C/KDN}$, $Atm^{-/-}$, $Atm^{+/-}$, and $Atm^{KD/-}$ ES cells. The small amount of protein detectable in the $Atm^{-/-}$ lane likely arises from slight contamination of the ES cells used for this analysis with WT fibroblasts from the feeder layer. (B) Fold increase of cell number relative to day 0, as measured by modified MTT assay (Sigma-Aldrich) in WT, $Atm^{-/-}$, and $Atm^{KD/-}$ ES cells under normal growth conditions. Three independent experiments were performed in two independently derived $Atm^{KD/-}$ ES cell lines. The graph and the error bars represent standard deviation derived from quadruplicated cultures in one representative experiment. (C) Frequency of metaphases with cytogenetic abnormalities in T-FISH analyses of WT, $Atm^{+/-}$, and $Atm^{KD/-}$ ES cells. The p-value (0.035) is obtained with χ^2 test. (D) The frequency of chromatid and chromosome breaks measured by T-FISH analyses in WT, $Atm^{+/-}$, and $Atm^{KD/-}$ ES cells. The χ^2 test p-value for the frequency of chromatid breaks between $Atm^{+/-}$ and $Atm^{KD/-}$ ES cells is 0.002 and for chromosome breaks is 0.101. (C and D) The error bars represent the standard deviations of multiple independent experiments. (E) Summary of cytogenetic abnormalities in WT, $Atm^{+/-}$, and $Atm^{KD/-}$ ES cells and controls. Ab, abnormal; MP, metaphase; Chs., chromosome; Cht., chromatid; Br, break; Std.Er, standard error. The data summarize the results from three or more independent experiments using at least two independently derived cell lines of each genotype. 20 metaphases were analyzed per line per experiment.

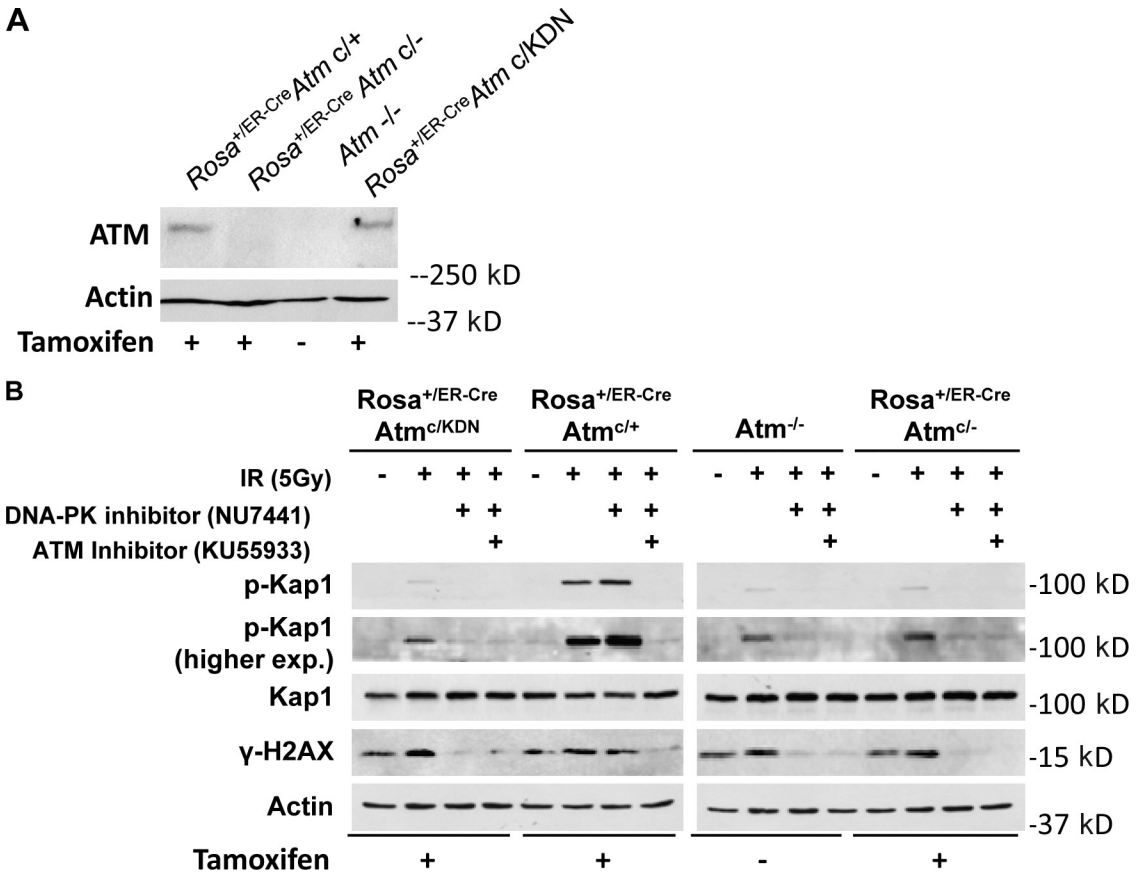

Figure 3. **ATM^{KD} is catalytically inactive.** (A) Western blot for total ATM protein in thymocytes from tamoxifen-treated *Rosa*$^{+/ER\text{-}Cre}$*Atm*$^{+/C}$, *Atm*$^{C/C}$, or *Atm*$^{C/KDN}$ mice and control *Atm*$^{-/-}$ mice. (B) Western blot for phosphorylated H2AX, phosphorylated KAP-1, and total KAP-1 and Actin in irradiated thymocyte (5 Gy) with or without preincubation with 15 µM ATM kinase inhibitor (KU55933; Tocris Bioscience) or 5 µM DNA-PKcs kinase inhibitor (NU7441; Tocris Bioscience). Cell lysates were collected 2 h after irradiation. Primary antibodies were used at the following dilutions: anti-Actin (1:10,000; Sigma-Aldrich), anti-ATM (1:500; MAT3; Sigma-Aldrich), anti–γ-H2AX (1:1,000; EMD Millipore), anti–KAP-1 (1:1,000; Cell Signaling Technology), antiphospho–KAP-1 (S824; 1:1,000; Bethyl Laboratories, Inc.). exp., exposure.

cells. Although it is unclear whether the effects of ATM kinase inhibitors on DNA repair are the same as those observed in *Atm*$^{KD/-}$ cells, our findings emphasize the need to distinguish the effects of ATM deletion and kinase inhibition in future studies.

The effect of ATM-KD protein on lymphocyte development

To test the consequences of ATM-KD protein expression in somatic cells, we generated *Rosa*$^{+/ER\text{-}Cre}$*Atm*$^{C/KDN}$ mice. The ROSA26-ER-Cre (*Rosa*$^{+/ER\text{-}Cre}$) allele ubiquitously expresses a tamoxifen-inducible fusion protein of estrogen receptor ligand-binding domain and Cre recombinase (ER-Cre) under the endogenous *Rosa26* promoter (de Luca et al., 2005; Guo et al., 2007). Lymphocyte development was then analyzed in conditional ATM-KD (*Rosa*$^{+/ER\text{-}Cre}$*Atm*$^{C/KDN}$), conditional ATM-null (*Rosa*$^{+/ER\text{-}Cre}$*Atm*$^{C/C(-)}$), and control (*Rosa*$^{+/ER\text{-}Cre}$*Atm*$^{C/+}$) mice 10 d after oral tamoxifen administration, at which time Cre-mediated recombination of the *Atm*^{C} and *Atm*^{KDN} alleles was readily observed in bone marrow, thymus, and spleen (Fig. S3). Western blot of total thymocytes showed that ATM-KD protein is expressed at levels similar to WT protein in thymocytes (Fig. 3 A). Upon irradiation, the levels of phosphorylated KAP-1 and H2AX (γ-H2AX) in thymocytes purified from tamoxifen-treated *Rosa*$^{+/ER\text{-}Cre}$*Atm*$^{C/KDN}$ mice was comparable to those from *Rosa*$^{+/ER\text{-}Cre}$*Atm*$^{C/C}$ mice, confirming the loss of ATM kinase activity in *Atm*$^{KD/-}$ thymocytes (Fig. 3 B). Compared with WT controls ($182 \pm 27 \times 10^6$), the total thymocyte number in tamoxifen-treated *Rosa*$^{+/ER\text{-}Cre}$*Atm*$^{C/KDN}$ mice ($60 \pm 17 \times 10^6$) was reduced to a level similar to *Rosa*$^{+/ER\text{-}Cre}$*Atm*$^{C/C}$ ($54 \pm 12 \times 10^6$) and *Atm*$^{-/-}$ ($42 \pm 16 \times 10^6$) mice ($n > 3$ for each group). FACS analyses of tamoxifen-treated *Rosa*$^{+/ER\text{-}Cre}$*Atm*$^{C/KDN}$ mice revealed thymocyte developmental defects, namely decreased TCR-β surface expression and decreased single-positive percentage in the thymus, comparable to those of tamoxifen-treated *Rosa*$^{+/ER\text{-}Cre}$*Atm*$^{C/C}$ or *Atm*$^{-/-}$ mice (Fig. 4 A; Borghesani et al., 2000). Together these data suggest that KD ATM protein partially blocks T cell development and, by extension, chromosomal V(D)J recombination to a level comparable with the absence of ATM protein.

Similarly, B cell development in tamoxifen-treated *Rosa*$^{+/ER\text{-}Cre}$*Atm*$^{C/KDN}$ mice was largely comparable with that of *Atm*$^{-/-}$ mice (Fig. 4 A). To test the effect of ATM-KD protein in CSR, we incubated partially purified (CD43^{-}) *Atm*$^{KD/-}$ and control splenic B cells with anti-CD40 plus IL-4 (interleukin 4) for 4 d to stimulate CSR to IgG1. PCR and Southern blot analyses confirmed the disappearance of *Atm*^{C} and

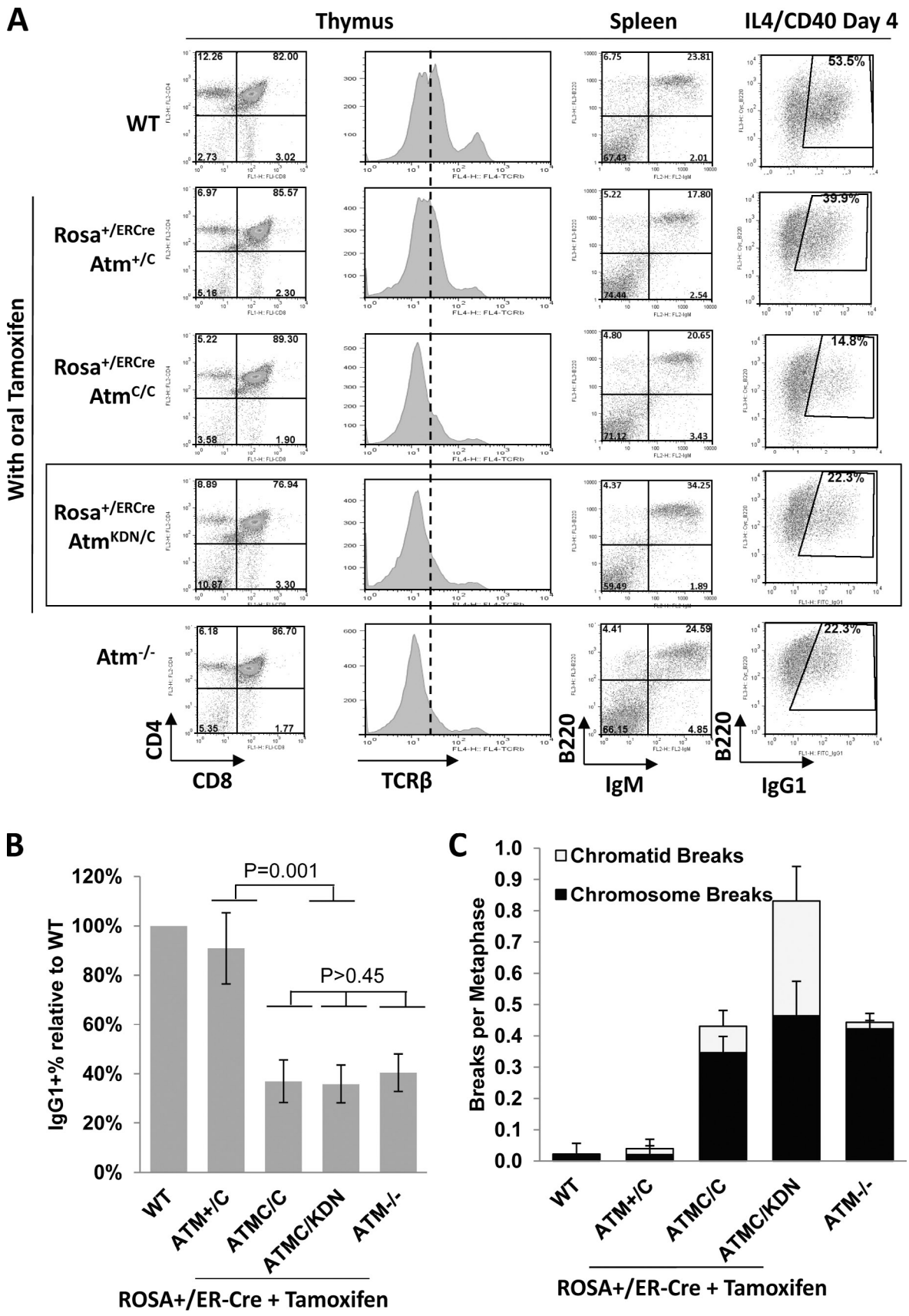

Figure 4. **Analysis of ATM KD lymphocytes.** (A) Representative flow cytometric analyses of total thymocytes stained with CD4, CD8, and TCR-β, and total splenocytes stained with B220 and IgM surface markers. For the B220/IgG$_1$ marker staining, CD43$^-$ splenocytes were isolated and stimulated in culture with anti-CD40 and IL-4 for 4 d before staining. A total of five independent experiments were performed, and one set of representative FACS analyses is shown. The dotted line shows the median level of surface TCR-β levels in WT thymocytes. The box highlights the analyses of

Atm^{KDN} alleles and the appearance of the recombined Atm^{-} and Atm^{KD} alleles in purified B cells (Fig. S3, A–C). Western analysis for phosphorylated H2AX (γ-H2AX) in irradiated B cells purified from tamoxifen-treated $Rosa^{+/ER\text{-}Cre}Atm^{C/KDN}$ and $Rosa^{+/ER\text{-}Cre}Atm^{C/C}$ mice confirmed the loss of ATM kinase activity in stimulated B cells (Fig. S3 D). Furthermore, B cells from tamoxifen-treated $Rosa^{+/ER\text{-}Cre}Atm^{C/C(-)}$ mice performed CSR at ∼40% of WT levels with increased genomic instability, similar to those of germline $Atm^{-/-}$ mice (Fig. 4, B and C; and Fig. S3), confirming functional loss of ATM protein in B cells from tamoxifen-treated $Rosa^{+/ER\text{-}Cre}Atm^{C/C(-)}$ mice. Nevertheless, B cells from tamoxifen-treated $Rosa^{+/ER\text{-}Cre}Atm^{C/KDN}$ mice underwent CSR at levels comparable with their ATM-null counterparts (Fig. 4 B and Fig. S3). Consistent with our findings on $Atm^{KD/-}$ ES cells, activated B cells from tamoxifen-treated $Rosa^{+/ER\text{-}Cre}Atm^{C/KDN}$ mice accumulated greater genomic instability, especially chromatid breaks, than $Atm^{-/-}$ B cells upon activation (Fig. 4 C and Fig. S3, D and E). Together, those results support the conclusion that the ATM-KD protein inhibits DNA repair in S and G2 phase of cell cycles.

Although NHEJ plays critical roles in lymphocyte-specific DSB repair events, it is largely dispensable for embryonic development (Lieber, 2010). In contrast, most HR factors are required for embryonic development. In this context, the embryonic lethality of $Atm^{KD/KD}$, but not $Atm^{-/-}$, mice may reflect an inhibitory function of ATM-KD protein in a subset of HR. Consistent with this hypothesis, the most dramatic increase of general genomic instability in $Atm^{KD/-}$ cells over ATM-null cells is chromatid breaks, which are typically associated with defects in S and G2 phase DNA repair.

ATM belongs to the family of phosphoinositide 3-kinase–related kinase, which also includes DNA-dependent protein kinase catalytic subunit (PKcs) and ATR. Although ATR is activated by RPA-coated single-strand DNA (Shiotani and Zou, 2009; Liu et al., 2011), ATM and DNA-PKcs are both activated by DNA DSBs, phosphorylate an overlapping pool of substrates (e.g., H2AX, KAP1, and p53; Callén et al., 2009b; Zha et al., 2011a,b), and have redundant functions during embryonic development and DNA repair (Gurley and Kemp, 2001; Sekiguchi et al., 2001; Callén et al., 2009b; Gapud et al., 2011; Zha et al., 2011b). It is possible that the presence of an enzymatically inactive ATM protein might prevent DNA-PKcs, and potentially other phosphoinositide 3-kinase–related kinases, from phosphorylating shared substrates, thereby disrupting DNA repair to a greater extent than complete loss of ATM alone. Loss of both ATM and DNA-PKcs led to CSR defects more severe than loss of either kinase alone (Callén et al., 2009b), but $Atm^{KD/-}$ and $Atm^{-/-}$ B cells performed CSR at similar levels (Fig. 4, A and B), inconsistent with inhibition of DNA-PKcs function in $Atm^{KD/-}$ B cells. Moreover, H2AX and KAP-1, two shared substrates of ATM and DNA-PKcs, are phosphorylated at comparable levels in $Atm^{KD/-}$ and $Atm^{-/-}$ B and T cells (Fig. 3 B and Fig. S3 D). Although phosphorylation of particular substrates of DNA-PKcs or DNA-PKcs itself may be inhibited in $Atm^{KD/-}$ cells, but not $ATM^{-/-}$ cells, our findings are inconsistent with global inhibition of DNA-PKcs activity in $Atm^{KD/-}$ cells. In this context, loss of ATM phosphorylation sites on DNA-PKcs leads to more severe defects in DNA repair than DNA-PKcs–null mice (Zhang et al., 2011).

Past studies of ATM function in DNA repair have focused primarily on its kinase activity. Here, we and others have shown that KD ATM proteins cause early embryonic lethality despite the normal embryonic development in the complete absence of ATM protein (see Daniel et al. in this issue). We further show that $Atm^{KD/-}$ ES and B cells accumulate much higher levels of chromosome instability, particularly chromatid breaks, relative to ATM-null cells. Despite the increased genomic instability, $Atm^{KD/-}$ lymphocytes performed V(D)J recombination and CSR at levels comparable with ATM-null cells. Together, these data suggest that although loss of ATM kinase activity and ATM-mediated phosphorylation of downstream targets compromise both NHEJ and, to a lesser extent, HR function, the ATM-KD protein elicits additional inhibitory effects in postreplication DNA repair, potentially HR. By uncovering unexpected functions for ATM protein in DNA repair and embryonic development, our study raises clinically relevant questions about the mechanism of ATM activation and the application of ATM kinase inhibitors.

Materials and methods

Generation of the ATM-KD allele

The DNA sequence for homologous targeting at the Atm locus was generated via PCR from TC1 ES cell DNA (129 strain). A targeting construct was designed to insert a NeoR gene cassette oriented in the opposite transcriptional direction from the endogenous *Atm* promoter into intron 57 next to the D2880A/N2885K mutation in exon 58. A 3.5-kb 5′ arm and 5.1-kb 3′ arm were PCR generated separately, cloned into the pBK vector, and sequenced. The 5′ arm was directly subcloned into pLNTK in the desired orientation. The mutation was introduced into the 3′ arm using site-directed mutagenesis and confirmed by sequencing. The mutated 3′ arm was then subcloned into pLNTK. The targeting construct was then electroporated into CSL3 ES cells (129 strain), and successful targeting was determined via Southern blot analyses using EcoRV-digested genomic DNA and a 5′ genomic probe as outlined in Fig. 1 B. The WT band is ∼22 kb, and the targeting introduced an additional EcoRV site and reduced the band to ∼4.7 kb. The corrected clones were confirmed with a 3′ probe with EcoRV digestions. Six independently targeted clones were sequenced for the ATM-KD mutation, and four were verified with correct mutations. Two were injected for germline transmission.

Mice

$Atm^{C/C}$ and $Rosa^{+/ER\text{-}Cre}$ mice were previously characterized (de Luca et al., 2005; Guo et al., 2007; Zha et al., 2008, 2011b). To activate Cre recombination, $Rosa^{+/ER\text{-}Cre}$ mice were orally fed with tamoxifen (5 mg in 90 µl of sunflower oil and 10 µl ethanol per mouse) daily for a consecutive 2 d.

$ATM^{KD/-}$ lymphocytes. (B) Relative frequency of the IgG1$^+$ cells among all B220$^+$ B cells (relative to WT cells in each experiments) in $Atm^{-/-}$ and $Atm^{KD/-}$ B cells. The data represent the mean and standard deviation from at least five experiments. The χ^2 test p-values are marked in the graph. (C) The frequency (per metaphase) of chromatid and chromosome breaks measured by T-FISH analyses in stimulated B cells from WT, $Atm^{-/-}$ mice, or tamoxifen-treated $Rosa^{+/ER\text{-}Cre}Atm^{+/C}$, $Atm^{C/C}$, or $Atm^{C/KDN}$ mice. The χ^2 test p-value for the frequency of chromatid breaks between $Atm^{+/-}$ and $Atm^{KD/-}$ B cells is 0.007 and for chromosome breaks is 0.816. The table summarized the data obtained from independent experiments performed on two or three mice of each genotype (see also Fig. S3 F).

The mice were analyzed 10–14 d after the second treatment. All animal experiments were conducted in a pathogen-free facility and approved by the Institute Animal Care and Use Committee of Columbia University.

Derivation of ES cells from mice

3–4-wk-old female $Atm^{+/KDN}$ mice were superovulated by intraperitoneal injection of 5.0 IU pregnant mare serum gonadotropin followed by intraperitoneal injection of 5.0 IU human chorionic gonadotropin (hCG; Sigma-Aldrich) 46–48 h later. The females were set up with adult male $Atm^{C/C}$ mice (1:1 ratio) immediately after the hCG injection. 4 d after the hCG injection, the mated females were sacrificed, and mature blastocysts were flushed out of the uterus and plated one per well in 96-well plates containing irradiated feeders. After 9–14-d incubation, the cells were expanded to 24-well plates, at which stage, half of the cells were frozen down, and the rest of the cells were used to derive DNA for genotyping. $Atm^{KDN/C}$ ES cells were then identified by PCR.

Cytogenetic analysis for genomic instability

ES cells, not grown on feeders, were plated 24 h before the addition of colcemid (KaryoMAX Colcemid Solution; Gibco) at 100 ng/ml for 1–2 h. ES cells were harvested by trypsinization, and metaphases were prepared as previously described (Zha et al., 2008, 2011b). T-FISH was performed as previously described (Franco et al., 2006). In brief, telomeres were stained with a Cy3-labled $(CCCTAA)_3$ peptide nucleic acid probe (Biosynthesis, Inc.), and DNA was counterstained with DAPI-containing mounting media (Vectashield; Vector Laboratories). Images were acquired using a microscope (Eclipse 80i; Nikon) with remote focus accessory and with a camera unit (CoolSNAP HQ; Photometrics) with the Plan Fluor lens (60 and 100×/1.30 NA oil; Nikon) in room temperature. All images were processed with NIS-Elements AR (version 3.10; Nikon). Chromosome breaks were defined by loss of telomere signal from both sister chromatids. Chromatid breaks were defined by loss of telomere signal from one of the two sister chromatids or a clearly broken DAPI signal in the middle of one chromatid (Fig. S2 C). We note that chromosomal gaps could not be reliably identified with the T-FISH assay; therefore, it is possible that the actual frequency of chromatid or chromosome breaks might be even higher than estimated.

Lymphocyte development and CSR

Lymphocyte populations were analyzed by flow cytometry as previously described (Li et al., 2008). Isolation and activation of splenic B cells and flow cytometric assays were performed as previously described (Li et al., 2008). In brief, $CD43^-$ splenic B cells were purified from total spleen using anti–mouse CD43 MACS beads following the manufacturer's instructions (Miltenyi Biotec). To stimulate the cells for CSR, the cells were incubated with α-CD40 plus IL-4 for 4 d, and the percentage of CSR to IgG1 was determined by surface staining and FACS analysis (Li et al., 2008). To assay for genomic instability, colcemid was added to a fraction of day 4 stimulated B cells for 4 h, and the metaphases were prepared and stained for T-FISH as described for ES cells.

Generation of mEOS2-ATM plasmids

To investigate the accumulation of ATM-WT and ATM-KD at sites of DNA damage in A-T cells, mEOS2-ATM expression constructs were generated. Plasmid pRSETa mEos2 was obtained from Addgene, and mEOS2 (McKinney et al., 2009) was amplified by PCR using primers with NotI linkers. The amplified sequence was inserted into pcDNA3-ATM-WT (Canman et al., 1998) at the NotI site, and plasmids with mEOS2 were inserted in the correct orientation identified by sequencing. mEOS2-ATM-WT Δ3′ untranslated and mEOS2-ATM-KD Δ3′ untranslated were generated by removing the ATM kinase domain and 3′ untranslated sequence in the original pcDNA3-ATM-WT by digestion with BlpI and XhoI and replacing with either the pcDNA3-ATM kinase-inactive sequence containing mutations at D2870A/N2875K (Canman et al., 1998) or the ATM-WT sequence, from which the 3′ end has been deleted, as described previously (Gamper et al., 2012). The expression of recombinant mEOS2-ATM protein is not disrupted by a small hairpin RNA that targets the 3′ untranslated sequence of the endogenous mRNA (Gamper et al., 2012).

Online supplemental material

Fig. S1 shows that the gross weight and lymphocyte development of $Atm^{+/KD}$ mice are comparable with $Atm^{+/+}$ littermates. Fig. S2 shows that the ATM-KD protein could be normally recruited to the site of DNA damage, and it also shows the representative images of T-FISH analyses. Fig. S3 shows the specific and efficient conversion of Atm^C to Atm^- alleles in B cells from tamoxifen-treated $Rosa^{+/ER\text{-}Cre}$ mice. Table S1 shows the primers used for genotyping the Atm^C, Atm^-, Atm^{KDN}, and Atm^{KD} alleles. Online supplemental material is available at http://www.jcb.org/cgi/content/full/jcb.201204098/DC1.

We wish to thank Dr. Richard Baer and Jennifer Crowe for their critical reading and comments on our manuscript. We thank Frances Lee and Chen Li for their technical assistance.

This work was supported by grants CA158073 to S. Zha and CA148644 to C.J. Bakkenist. It is also supported by funding made available by St. Baldrick's Foundation, Gabrielle Angel Foundation, John Driscoll Jr. Children's Medical Award, and Leukemia Lymphoma Foundation to S. Zha. K. Yamamoto is partially supported by the graduate program of Pathobiology and Molecular Medicine at Columbia University. W. Jiang is supported in part by the National Institutes of Health/National Cancer Institute training grant T32-CA09503 to Herbert Irving Comprehensive Cancer Research Center at Columbia University.

Submitted: 18 April 2012
Accepted: 2 July 2012

References

Bakkenist, C.J., and M.B. Kastan. 2003. DNA damage activates ATM through intermolecular autophosphorylation and dimer dissociation. *Nature*. 421:499–506. http://dx.doi.org/10.1038/nature01368

Barlow, C., S. Hirotsune, R. Paylor, M. Liyanage, M. Eckhaus, F. Collins, Y. Shiloh, J.N. Crawley, T. Ried, D. Tagle, and A. Wynshaw-Boris. 1996. Atm-deficient mice: a paradigm of ataxia telangiectasia. *Cell*. 86: 159–171. http://dx.doi.org/10.1016/S0092-8674(00)80086-0

Barone, G., A. Groom, A. Reiman, V. Srinivasan, P.J. Byrd, and A.M. Taylor. 2009. Modeling ATM mutant proteins from missense changes confirms retained kinase activity. *Hum. Mutat.* 30:1222–1230. http://dx.doi.org/10.1002/humu.21034

Bhatti, S., S. Kozlov, A.A. Farooqi, A. Naqi, M. Lavin, and K.K. Khanna. 2011. ATM protein kinase: the linchpin of cellular defenses to stress. *Cell. Mol. Life Sci.* 68:2977–3006. http://dx.doi.org/10.1007/s00018-011-0683-9

Borghesani, P.R., F.W. Alt, A. Bottaro, L. Davidson, S. Aksoy, G.A. Rathbun, T.M. Roberts, W. Swat, R.A. Segal, and Y. Gu. 2000. Abnormal development of Purkinje cells and lymphocytes in Atm mutant mice. *Proc. Natl. Acad. Sci. USA*. 97:3336–3341. http://dx.doi.org/10.1073/pnas.050584897

Bredemeyer, A.L., G.G. Sharma, C.Y. Huang, B.A. Helmink, L.M. Walker, K. C. Khor, B. Nuskey, K.E. Sullivan, T.K. Pandita, C.H. Bassing, and B.P. Sleckman. 2006. ATM stabilizes DNA double-strand-break complexes during V(D)J recombination. *Nature*. 442:466–470. http://dx.doi.org/10.1038/nature04866

Callén, E., S. Bunting, C.Y. Huang, M.J. Difilippantonio, N. Wong, B. Khor, G. Mahowald, M.J. Kruhlak, T. Ried, B.P. Sleckman, and A. Nussenzweig. 2009a. Chimeric IgH-TCRalpha/delta translocations in T lymphocytes mediated by RAG. *Cell Cycle*. 8:2408–2412. http://dx.doi.org/10.4161/cc.8.15.9085

Callén, E., M. Jankovic, N. Wong, S. Zha, H.T. Chen, S. Difilippantonio, M. Di Virgilio, G. Heidkamp, F.W. Alt, A. Nussenzweig, and M. Nussenzweig. 2009b. Essential role for DNA-PKcs in DNA double-strand break repair and apoptosis in ATM-deficient lymphocytes. *Mol. Cell*. 34:285–297. http://dx.doi.org/10.1016/j.molcel.2009.04.025

Canman, C.E., D.S. Lim, K.A. Cimprich, Y. Taya, K. Tamai, K. Sakaguchi, E. Appella, M.B. Kastan, and J.D. Siliciano. 1998. Activation of the ATM kinase by ionizing radiation and phosphorylation of p53. *Science*. 281:1677–1679. http://dx.doi.org/10.1126/science.281.5383.1677

Carson, C.T., R.A. Schwartz, T.H. Stracker, C.E. Lilley, D.V. Lee, and M.D. Weitzman. 2003. The Mre11 complex is required for ATM activation and the G2/M checkpoint. *EMBO J.* 22:6610–6620. http://dx.doi.org/10.1093/emboj/cdg630

Daniel, J.A., M. Pellegrini, J.H. Lee, T.T. Paull, L. Feigenbaum, and A. Nussenzweig. 2008. Multiple autophosphorylation sites are dispensable for murine ATM activation in vivo. *J. Cell Biol.* 183:777–783. http://dx.doi.org/10.1083/jcb.200805154

Daniel, J.A., M. Pellegrini, B.-S. Lee, Z. Guo, D. Filsuf, N.V. Belkina, Z. You, T.T. Paull, B.P. Sleckman, L. Feigenbaum, and A. Nussenzweig. 2012. Loss of ATM kinase activity leads to embryonic lethality in mice. *J. Cell Biol.* 198:295–304.

Davis, A.J., S. So, and D.J. Chen. 2010. Dynamics of the PI3K-like protein kinase members ATM and DNA-PKcs at DNA double strand breaks. *Cell Cycle*. 9:2529–2536.

de Luca, C., T.J. Kowalski, Y. Zhang, J.K. Elmquist, C. Lee, M.W. Kilimann, T. Ludwig, S.M. Liu, and S.C. Chua Jr. 2005. Complete rescue of obesity, diabetes, and infertility in db/db mice by neuron-specific LEPR-B transgenes. *J. Clin. Invest.* 115:3484–3493. http://dx.doi.org/10.1172/JCI24059

Franco, S., M. Gostissa, S. Zha, D.B. Lombard, M.M. Murphy, A.A. Zarrin, C. Yan, S. Tepsuporn, J.C. Morales, M.M. Adams, et al. 2006. H2AX prevents DNA breaks from progressing to chromosome breaks and translocations. *Mol. Cell*. 21:201–214. http://dx.doi.org/10.1016/j.molcel.2006.01.005

Gamper, A.M., S. Choi, Y. Matsumoto, D. Banerjee, A.E. Tomkinson, and C.J. Bakkenist. 2012. ATM protein physically and functionally interacts with proliferating cell nuclear antigen to regulate DNA synthesis. *J. Biol. Chem.* 287:12445–12454. http://dx.doi.org/10.1074/jbc.M112.352310

Gapud, E.J., Y. Dorsett, B. Yin, E. Callen, A. Bredemeyer, G.K. Mahowald, K.Q. Omi, L.M. Walker, J.J. Bednarski, P.J. McKinnon, et al. 2011. Ataxia telangiectasia mutated (Atm) and DNA-PKcs kinases have overlapping activities during chromosomal signal joint formation. *Proc. Natl. Acad. Sci. USA*. 108:2022–2027. http://dx.doi.org/10.1073/pnas.1013295108

Gilad, S., R. Khosravi, D. Shkedy, T. Uziel, Y. Ziv, K. Savitsky, G. Rotman, S. Smith, L. Chessa, T.J. Jorgensen, et al. 1996. Predominance of null mutations in ataxia-telangiectasia. *Hum. Mol. Genet.* 5:433–439. http://dx.doi.org/10.1093/hmg/5.4.433

Guo, K., J.E. McMinn, T. Ludwig, Y.H. Yu, G. Yang, L. Chen, D. Loh, C. Li, S. Chua Jr., and Y. Zhang. 2007. Disruption of peripheral leptin signaling in mice results in hyperleptinemia without associated metabolic abnormalities. *Endocrinology*. 148:3987–3997. http://dx.doi.org/10.1210/en.2007-0261

Gurley, K.E., and C.J. Kemp. 2001. Synthetic lethality between mutation in Atm and DNA-PK(cs) during murine embryogenesis. *Curr. Biol.* 11:191–194. http://dx.doi.org/10.1016/S0960-9822(01)00048-3

Herzog, K.H., M.J. Chong, M. Kapsetaki, J.I. Morgan, and P.J. McKinnon. 1998. Requirement for Atm in ionizing radiation-induced cell death in the developing central nervous system. *Science*. 280:1089–1091.

Hickson, I., Y. Zhao, C.J. Richardson, S.J. Green, N.M. Martin, A.I. Orr, P.M. Reaper, S.P. Jackson, N.J. Curtin, and G.C. Smith. 2004. Identification and characterization of a novel and specific inhibitor of the ataxia-telangiectasia mutated kinase ATM. *Cancer Res.* 64:9152–9159.

Huang, C.-Y., G.G. Sharma, L.M. Walker, C.H. Bassing, T.K. Pandita, and B.P. Sleckman. 2007. Defects in coding joint formation in vivo in developing ATM-deficient B and T lymphocytes. *J. Exp. Med.* 204:1371–1381. http://dx.doi.org/10.1084/jem.20061460

Huber, A., P. Bai, J.M. de Murcia, and G. de Murcia. 2004. PARP-1, PARP-2 and ATM in the DNA damage response: functional synergy in mouse development. *DNA Repair (Amst.)*. 3:1103–1108.

Kennedy, R.D., C.C. Chen, P. Stuckert, E.M. Archila, M.A. De la Vega, L.A. Moreau, A. Shimamura, and A.D. D'Andrea. 2007. Fanconi anemia pathway-deficient tumor cells are hypersensitive to inhibition of ataxia telangiectasia mutated. *J. Clin. Invest.* 117:1440–1449.

Lakin, N.D., P. Weber, T. Stankovic, S.T. Rottinghaus, A.M. Taylor, and S.P. Jackson. 1996. Analysis of the ATM protein in wild-type and ataxia telangiectasia cells. *Oncogene*. 13:2707–2716.

Lavin, M.F. 2008. Ataxia-telangiectasia: from a rare disorder to a paradigm for cell signalling and cancer. *Nat. Rev. Mol. Cell Biol.* 9:759–769. http://dx.doi.org/10.1038/nrm2514

Lee, J.H., and T.T. Paull. 2004. Direct activation of the ATM protein kinase by the Mre11/Rad50/Nbs1 complex. *Science*. 304:93–96. http://dx.doi.org/10.1126/science.1091496

Lee, J.H., and T.T. Paull. 2005. ATM activation by DNA double-strand breaks through the Mre11-Rad50-Nbs1 complex. *Science*. 308:551–554. http://dx.doi.org/10.1126/science.1108297

Li, G., F.W. Alt, H.L. Cheng, J.W. Brush, P.H. Goff, M.M. Murphy, S. Franco, Y. Zhang, and S. Zha. 2008. Lymphocyte-specific compensation for XLF/cernunnos end-joining functions in V(D)J recombination. *Mol. Cell*. 31:631–640. http://dx.doi.org/10.1016/j.molcel.2008.07.017

Lieber, M.R. 2010. The mechanism of double-strand DNA break repair by the nonhomologous DNA end-joining pathway. *Annu. Rev. Biochem.* 79:181–211. http://dx.doi.org/10.1146/annurev.biochem.052308.093131

Liu, S., B. Shiotani, M. Lahiri, A. Maréchal, A. Tse, C.C. Leung, J.N. Glover, X.H. Yang, and L. Zou. 2011. ATR autophosphorylation as a molecular switch for checkpoint activation. *Mol. Cell*. 43:192–202. http://dx.doi.org/10.1016/j.molcel.2011.06.019

Lumsden, J.M., T. McCarty, L.K. Petiniot, R. Shen, C. Barlow, T.A. Wynn, H.C. Morse III, P.J. Gearhart, A. Wynshaw-Boris, E.E. Max, and R.J. Hodes. 2004. Immunoglobulin class switch recombination is impaired in *Atm*-deficient mice. *J. Exp. Med.* 200:1111–1121. http://dx.doi.org/10.1084/jem.20041074

McKinney, S.A., C.S. Murphy, K.L. Hazelwood, M.W. Davidson, and L.L. Looger. 2009. A bright and photostable photoconvertible fluorescent protein. *Nat. Methods*. 6:131–133. http://dx.doi.org/10.1038/nmeth.1296

Ménisser-de Murcia, J., M. Mark, O. Wendling, A. Wynshaw-Boris, and G. de Murcia. 2001. Early embryonic lethality in PARP-1 Atm double-mutant mice suggests a functional synergy in cell proliferation during development. *Mol. Cell. Biol.* 21:1828–1832. http://dx.doi.org/10.1128/MCB.21.5.1828-1832.2001

Murga, M., S. Bunting, M.F. Montaña, R. Soria, F. Mulero, M. Cañamero, Y. Lee, P.J. McKinnon, A. Nussenzweig, and O. Fernandez-Capetillo. 2009. A mouse model of ATR-Seckel shows embryonic replicative stress and accelerated aging. *Nat. Genet.* 41:891–898. http://dx.doi.org/10.1038/ng.420

O'Gorman, S., N.A. Dagenais, M. Qian, and Y. Marchuk. 1997. Protamine-Cre recombinase transgenes efficiently recombine target sequences in the male germ line of mice, but not in embryonic stem cells. *Proc. Natl. Acad. Sci. USA*. 94:14602–14607. http://dx.doi.org/10.1073/pnas.94.26.14602

Pellegrini, M., A. Celeste, S. Difilippantonio, R. Guo, W. Wang, L. Feigenbaum, and A. Nussenzweig. 2006. Autophosphorylation at serine 1987 is dispensable for murine Atm activation in vivo. *Nature*. 443:222–225. http://dx.doi.org/10.1038/nature05112

Rainey, M.D., M.E. Charlton, R.V. Stanton, and M.B. Kastan. 2008. Transient inhibition of ATM kinase is sufficient to enhance cellular sensitivity to ionizing radiation. *Cancer Res.* 68:7466–7474. http://dx.doi.org/10.1158/0008-5472.CAN-08-0763

Reina-San-Martin, B., H.T. Chen, A. Nussenzweig, and M.C. Nussenzweig. 2004. ATM is required for efficient recombination between immunoglobulin switch regions. *J. Exp. Med.* 200:1103–1110. http://dx.doi.org/10.1084/jem.20041162

Rooney, S., J. Chaudhuri, and F.W. Alt. 2004. The role of the non-homologous end-joining pathway in lymphocyte development. *Immunol. Rev.* 200:115–131. http://dx.doi.org/10.1111/j.0105-2896.2004.00165.x

Sekiguchi, J., D.O. Ferguson, H.T. Chen, E.M. Yang, J. Earle, K. Frank, S. Whitlow, Y. Gu, Y. Xu, A. Nussenzweig, and F.W. Alt. 2001. Genetic interactions between ATM and the nonhomologous end-joining factors in genomic stability and development. *Proc. Natl. Acad. Sci. USA*. 98:3243–3248. http://dx.doi.org/10.1073/pnas.051632098

Shiotani, B., and L. Zou. 2009. Single-stranded DNA orchestrates an ATM-to-ATR switch at DNA breaks. *Mol. Cell*. 33:547–558. http://dx.doi.org/10.1016/j.molcel.2009.01.024

Uziel, T., Y. Lerenthal, L. Moyal, Y. Andegeko, L. Mittelman, and Y. Shiloh. 2003. Requirement of the MRN complex for ATM activation by DNA damage. *EMBO J.* 22:5612–5621. http://dx.doi.org/10.1093/emboj/cdg541

White, J.S., S. Choi, and C.J. Bakkenist. 2008. Irreversible chromosome damage accumulates rapidly in the absence of ATM kinase activity. *Cell Cycle*. 7:1277–1284. http://dx.doi.org/10.4161/cc.7.9.5961

White, J.S., S. Choi, and C.J. Bakkenist. 2010. Transient ATM kinase inhibition disrupts DNA damage-induced sister chromatid exchange. *Sci. Signal.* 3:ra44. http://dx.doi.org/10.1126/scisignal.2000758

Williams, B.R., O.K. Mirzoeva, W.F. Morgan, J. Lin, W. Dunnick, and J.H. Petrini. 2002. A murine model of Nijmegen breakage syndrome. *Curr. Biol.* 12:648–653. http://dx.doi.org/10.1016/S0960-9822(02)00763-7

Xu, Y., and D. Baltimore. 1996. Dual roles of ATM in the cellular response to radiation and in cell growth control. *Genes Dev.* 10:2401–2410. http://dx.doi.org/10.1101/gad.10.19.2401

Zha, S., J. Sekiguchi, J.W. Brush, C.H. Bassing, and F.W. Alt. 2008. Complementary functions of ATM and H2AX in development and suppression of genomic instability. *Proc. Natl. Acad. Sci. USA*. 105:9302–9306. http://dx.doi.org/10.1073/pnas.0803520105

Zha, S., C. Guo, C. Boboila, V. Oksenych, H.L. Cheng, Y. Zhang, D.R. Wesemann, G. Yuen, H. Patel, P.H. Goff, et al. 2011a. ATM damage response and XLF repair factor are functionally redundant in joining DNA breaks. *Nature*. 469:250–254. http://dx.doi.org/10.1038/nature09604

Zha, S., W. Jiang, Y. Fujiwara, H. Patel, P.H. Goff, J.W. Brush, R.L. Dubois, and F.W. Alt. 2011b. Ataxia telangiectasia-mutated protein and DNA-dependent protein kinase have complementary V(D)J recombination functions. *Proc. Natl. Acad. Sci. USA*. 108:2028–2033. http://dx.doi.org/10.1073/pnas.1019293108

Zhang, S., H. Yajima, H. Huynh, J. Zheng, E. Callen, H.T. Chen, N. Wong, S. Bunting, Y.F. Lin, M. Li, et al. 2011. Congenital bone marrow failure in DNA-PKcs mutant mice associated with deficiencies in DNA repair. *J. Cell Biol.* 193:295–305. http://dx.doi.org/10.1083/jcb.201009074